Appl.Catal.A: General 282 (2005) 135-145

Carbon accumulation, deactivation and reactivation of Pt catalysts upon exposure to hydrocarbons

Z. Paál[a,b], A. Wootsch[a], R. Schlögl[b], U. Wild[b]

[a]Institute of Isotopes, Chemical Research Center, Hungarian Academy of Sciences, P.O. Box 77, Budapest H-1525, Hungary
[b]Fritz-Haber-Institut der MPG, Faradayweg 4-6, D-14195 Berlin, Germany

* Corresponding author: Tel.: +36 1 392 2531; fax: +36 1 392 2533,

Received: 21 October 2004,; revised 7 December 2004; accepted 8 December 2004; Published Online: 21 January 2005

Abstract

The formation and catalytic effect of carbonaceous deposits was studied on monofunctional Pt catalysts: Pt black (PtN, i.e., reduced with hydrazine), Pt/SiO_2 (EUROPT-1), Pt on "herringbone" graphite nanofiber (Pt/GNF-H, GNF being able to store hydrogen) and Pt/CeO_2 (ceria tending to consume spilt over hydrogen). They were exposed to hexane or *t,t*-hexa-2,4-diene between 483 and 663 K, with or without H_2. Hydrocarbon transformations during these *deactivating exposures* as well as in subsequent *standard test reaction* with hexane in hydrogen excess were studied. Carbon accumulation on Pt black after analogous deactivating treatments was also examined by electron spectroscopy (XPS and UPS). The abundance of hydrogen on Pt sites controlled the activity and selectivity containing much Pt—C species. The amount of surface C could reach ~45% causing almost total activity loss, but even ~30% C on Pt blacks decreased markedly the catalytic activity, due to massive 3D deposits. "Disordered" carbon selectively poisoned the formation of saturated C_6 products and fragmentation. The yield of dehydrogenation to hexenes was a good universal indicator of deactivation for each catalyst. Four regions were distinguished: "beneficial", "selective", "non-selective" and "severe" deactivation.

Keywords: Pt; Platinum black; Monofunctional Pt; Deactivation; Hexane; Hydrogen; Aromatization; Isomerization; XPS; UPS

1. Introduction

Carbonaceous entities have been shown to be present on Pt catalysts during "skeletal" hydrocarbon reactions [1] and [2]. Somorjai [1] distinguished ordered or disordered three-dimensional (3D) carbonaceous polymers and individual C atoms attached to Pt atoms ("Pt—C") and assumed that clean Pt islands present would do the catalytic reactions. Some of the "massive" coke detected by electron spectroscopy, may have formed during evacuation [3] dehydrogenating the "hydrocarbonaceous deposits", always present during reactions of hydrocarbon–H_2 mixtures [1] and [4]. Graphitic moieties, poly-C_xH_y as well as "Pt—C", were observed by XPS and UPS after treating Pt black samples with hydrocarbons at reaction temperatures [5] and [6].

Regeneration of Pt black and accumulation of carbonaceous residues were accompanied also by restructuring of Pt black crystallites [7], supporting the "flexible surface" concept [8] and [9]. X-ray diffraction (XRD) showed more intense (3 1 1) and (2 2 0) reflections (so-called "B_5" structures) on hydrogen-treated Pt [10]. These structures favored skeletal rearrangement reactions [11] and [12] such as isomerization and/or C_5-cyclization [13] and [14]. Exposing even a single (1 1 1) crystal surface to H_2 initiated restructuring of stepped surfaces [15] to form so-called "B_5" structures, more active in skeletal hydrocarbon reactions [1], [11], [12] and [16].

The catalysts were exposed to hydrocarbons in the presence and absence of hydrogen. The product composition was monitored after these "*deactivating exposures*" as well as in subsequent *standard test reactions* with hexane–H_2 mixture at $T = 603$ K. The surface of Pt during alkane

reactions is covered by chemisorbed hydrogen and dissociated alkane radicals [2] and [4], which may give either reaction products or dehydrogenate further to form carbonaceous deposits [17] and [18]. More hydrogen favored isomerization and C_5-cyclization [13], while less hydrogen promoted hydrogenolysis and aromatization as well as coking [19]. The "virtual surface hydrogen pressure" may be higher than that in the gas phase [20], [21] and [22].

The present study will report on the effect of two deactivating hydrocarbons: hexane (*n*H) and *trans-trans*-hexa-2,4-diene (2,4HD$=\!=$) alone or with a six-fold excess of H_2 in a wide temperature range (483–663 K). The effect(s) of the unsaturated and saturated deactivated agents in the presence (and also in the absence) of hydrogen will be compared using Pt black as well as three monofunctional supported Pt catalysts: Pt/SiO_2 (the well-known and much used EUROPT-1 [23] and [24]) Pt on a graphite-nanofiber (GNF) support [25] and Pt/CeO_2 [26]. The latter supports exhibited opposite behavior towards spilt over hydrogen: GNF stored it whereas ceria reacted with hydrogen to give Ce^{III}. Two parallel exposures were carried out with Pt black: (1) in the preparation chamber of an UHV apparatus, followed by XPS and UPS measurements; (2) in a catalytic reactor using exactly the same mixtures. Catalytic properties were monitored (a) during deactivating runs and (b) in standard test runs after deactivation. The changes in activities and selectivities during skeletal reactions of hexane will be used for characterization of the surface state, and discussed together with surface analysis of Pt black. Common features and differences of monofunctional Pt catalysts will be pointed out. This paper will also sum up the experience obtained by several years' research work in analogous field [6], [7], [27],[28] and [29].

2. Experimental

2.1. Catalysts

Pt black was prepared by reduction from aqueous solution of H_2PtCl_6 with hydrazine [30], denoted as PtN. Its BET surface was 2.34 $m^2\ g^{-1}$, dispersion $D = 0.9\%$ [20]. The results obtained with another Pt black (Pt–HCHO, BET surface, 2.64 $m^2\ g^{-1}$, dispersion $D = 1.6\%$ [6]) were very similar, thus they will not be tackled in detail here. The supported catalysts were: 6% Pt/SiO_2, known as EUROPT-1 [23], $D = 60\%$; 2%; Pt/CeO_2 calcined at 773 K, corresponding to 2Pt-Ce HTR in Ref. [26], $D = 35\%$. The graphite supported catalyst was 4% Pt on "herringbone-type" graphite-nanofiber, Pt/GNF-H [31]. It was synthesized by impregnating 0.5 g GNF-H support and adding the calculated amount of H_2PtCl_6 (2% solution in ethanol) to a 1:4 mixture of dry ethanol and toluene, stirred for 25 h, dried and reduced in H_2 flow at 473 K, then at 637 K [25]. The metal dispersion was 31% [32].

2.2. Electron spectroscopy

XPS and UPS were measured by a Leybold LHS 12 MCD instrument as described earlier [6], [7] and [27]. UPS used He I (21.2 eV), pass energy (PE) = 6 eV or He II excitation (40.8 eV), PE = 12 eV. An Mg Kα anode was used for XPS (PE = 48 eV). Atomic compositions (O 1s, C 1s, Pt 4f) were determined from peak areas using literature sensitivity factors [33] assuming a homogeneous composition model.

2.3. Carbonizing runs ("pretreatments")

Mixtures of 13 mbar of hydrocarbon, hexane (*n*H) or *trans*,*trans*-hexa-2,4-diene (2,4HD$=\!=$) and 80 mbar of hydrogen were introduced and kept over the catalyst, typically for 20 min. Similar runs were also carried out with 53 mbar hexane alone. The same exposures was done both in the preparation chamber of the electron spectrometer and in the catalytic glass reactor (see below). Contact with air was avoided between pretreatment and measurement in both cases.

2.4. Deactivating and test runs

The product composition was checked by gas chromatography, after the deactivating run of 20 min, as well as in "*standard test runs*" using a mixture of hexane (*n*H) and hydrogen at $p(nH):p(H_2) = 13:160$ mbar in the closed-loop circulation reactor [6] and [20]. The residual activity and selectivities were determined in samples taken after 5, 20, 35 and 50 min run time.

3. Results

3.1. Surface and structural analysis of Pt black

Electron spectroscopy (XPS and UPS) was carried out with Pt black only. An in situ hydrogen treatment removed most oxygen of the "as received" sample stored in air [7], [34] and [35]. The oxygen content remained typically below 5%. Regeneration with O_2 could decrease the amount of residual carbon below 10%. A subsequent H_2 treatment *increased* again the C percentage. We attributed this phenomenon to hydrogen penetrating into inter-atomic cavities, promoting this way, not only "hydrogen-induced rearrangement" [10] but also the segregation of "subsurface" carbon to the surface [7]. Exposures to hydrocarbons at lower temperatures resulted in much less carbon on the surface (Table 1). A pronounced difference appeared between *n*H and 2,4HD$=\!=$ treatments: the latter producing more surface carbon, with one exception: identical amount of C appeared after treatments at 483 K. Exposure to *n*H at

Table 1: Composition of Pt blacks after various treatments, as determined by XPS

Sample and treatment	T (K)	Composition (at.%)		
		Pt 4f	C 1s	O 1s
PtN				
H_2 of the "as is" sample	603	82	15	3
*n*H:H_2 = 13:80 mbar	483	78	22	1
*n*H:H_2 = 13:80 mbar	543	73	26	1
*n*H:H_2 = 13:80 mbar	603	70	27	3
*n*H:H_2 = 13:80 mbar	663	69	31	–
*n*H 53 mbar	603	59	40	1
24HD=:H_2 = 13:80 mbar	483	70	23	7
24HD=:H_2 = 13:80 mbar	543	65	33	2
24HD=:H_2 = 13:80 mbar	603	61	38	1
24HD=:H_2 = 13:80 mbar	663	55	45	–
Regeneration: O_2	603	89	9	2
H_2 after O_2	603	87	12	1

603 K *without* hydrogen gave still less surface C than 2,4HD═ *with* H_2 at 663 K.

In addition to the different amounts of accumulated carbon, its chemical state also showed characteristic changes after different treatments. Fig. 1 illustrates difference spectra between the carbon region measured on PtN treated with *n*H and 2,4HD═, respectively, from 483 to 663 K. The energy scale of all spectra was adjusted to the Pt 4f 7/2 line (71.1 eV) and the C 1s areas were normalized to the area of the Pt 4f doublet. The nearly equal carbon percentage after *n*H/H_2 and 2,4HD═/H_2 exposures at 483 K (Table 1) was present in different chemical states. The amount of "deactivating disordered carbon" (BE ~284.1 eV [6]) as well as that of the "graphite-like" C was higher after hexane treatment whereas some CO was observed after hexadiene exposure. CO is a minor component of the residual gas in the preparation chamber and may appear as a chemisorbed entity (cf. Fig. 9 in Ref. [7]). It was reported that CO is more weakly bound in the presence of carbonaceous deposits than on clean Pt [36] and Pd [37] surfaces. Thus, we believe that the appearance of surface CO can be taken as an indicator of the surface purity, i.e. the absence of strongly bonded carbon deposits. The higher amount of carbon deposited from 2,4HD═ appeared as positive peaks on the difference spectra (denoted as "HD–*n*H"). More C was present after pretreatments at higher temperature. It contained several carbon species: "deactivating carbon" (~284.1 eV), identified with the "disordered C" [1], "graphene" entities (~284.4 eV), graphite (~284.6 eV) as well as some C_xH_y polymer (~285.4 eV) [6]. Graphitization of carbon on Pt was confirmed also by electron microscopy [6]. One difference spectrum for Pt reduced with formaldehyde [6]. "Pt–HCHO" is also shown in Fig. 1. It was very similar to that measured for PtN. The Pt 4f spectra showed predominantly clean metallic Pt, as reported previously [6], [7] and [38], hence such spectra will not be presented here.

Fig. 2a compares He II UP spectra obtained after 2,4HD═/H_2 treatments at two temperatures, at 543 K and at 663 K (maximum carbon accumulation). Fig. 2b depicts He I spectra after 2,4HD═ and *n*H exposures at 603 K.

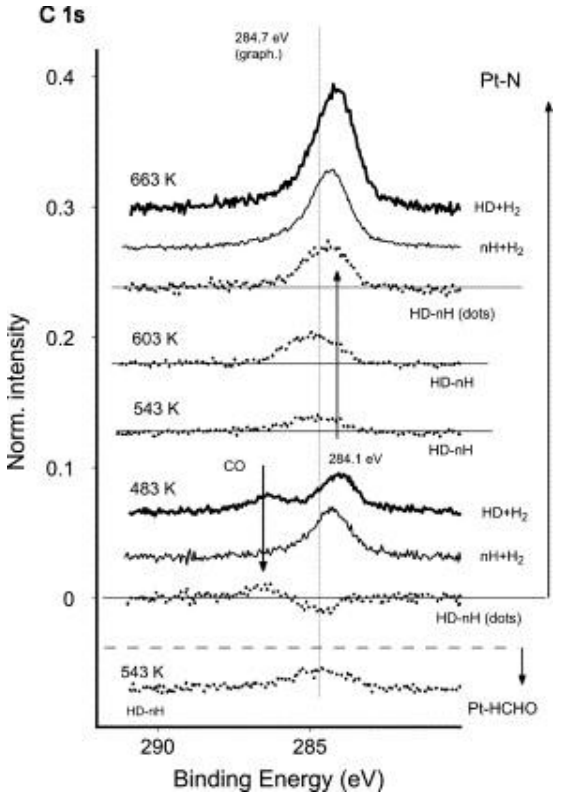

Fig. 1. C 1s region of the PtN catalyst treated with *n*H/H_2 and 2,4HD═/H_2 at different temperatures. The BE values of the spectra were adjusted to Pt 4f 7/2 = 71.1 eV and normalized according to the Pt 4f area. Difference spectra were calculated from these normalized spectra. Only these have been shown for treatments at 543 and 603 K. The lowest spectrum shows a similar difference spectrum measured for Pt–HCHO.

Applying higher temperature and 2,4HD═ rather than *n*H resulted in a quite featureless broad difference spectrum. It was more pronounced in He I (with shallower information depth) than in He II [28]. This shape is characteristic of an overlayer-type carbon deposition [6] and [7]. XPS confirmed its mainly graphitic character (cf. Fig. 1). The pronounced Fermi-edges verify that the carbon-free Pt surface was in clean metallic state in each case.

Fig. 2a compares He II UP spectra obtained after 2,4HD═/H_2 treatments at two temperatures, at 543 K and at 663 K (maximum carbon accumulation). Fig. 2b depicts He I spectra after 2,4HD═ and *n*H exposures at 603 K. Applying higher temperature and 2,4HD═ rather than *n*H resulted in a quite featureless broad difference spectrum. It was more pronounced in He I (with shallower information depth) than in He II [28]. This shape is characteristic of an overlayer-type carbon deposition [6] and [7]. XPS confirmed its mainly graphitic character (cf. Fig. 1). The pronounced Fermi-edges verify that the carbon-free Pt surface was in clean metallic state in each case.

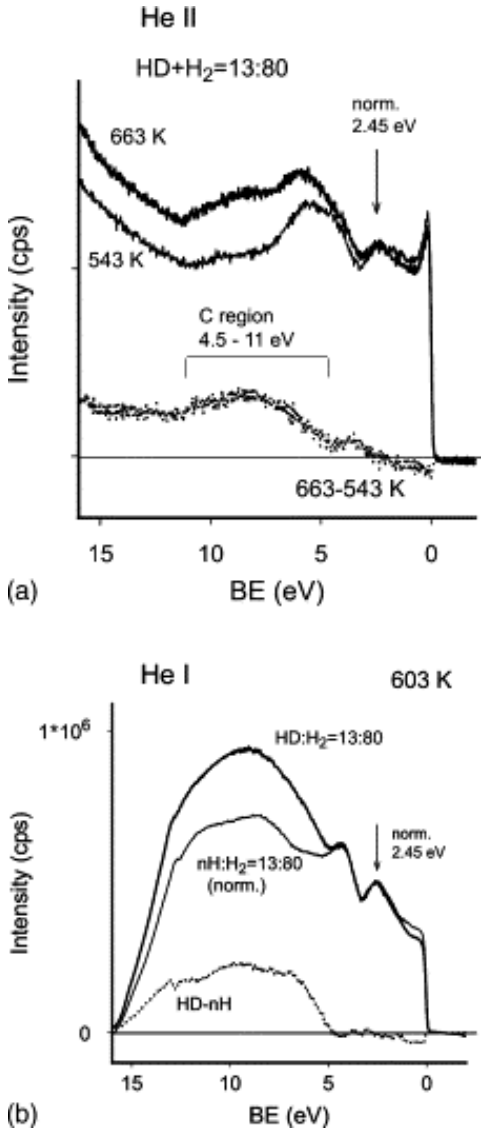

Fig. 2. Comparative UP spectra and their differences (after intensity normalization): (a) He II spectra after 2,4HD═/H_2 treatments at two temperatures; (b) He I spectra after *n*H/H_2 and 2,4HD═/H_2 treatments at 603 K.

X-ray diffraction spectra of PtN after two selected treatments (*n*H/H_2 at 483 K and *n*H alone at 603 K) are shown in Fig. 3. Deactivation with *n*H:H_2 = 13:80 mbar at 483 K, enhanced the (3 1 1) and (2 0 0) XRD reflections (Fig. 3), as observed after regenerative hydrogen treatments [29]. Thus, this exposure – resulting in less "massive carbon", cf Fig.1 – caused recrystallization typical for hydrogen-rich atmospheres. It is not clear if CO present (Fig. 1) contributed to this restructuring. Much carbon accumulated after the treatment with "*n*H alone" brought about changes in the opposite sense. These structural features may have contributed to the variation of catalytic properties.

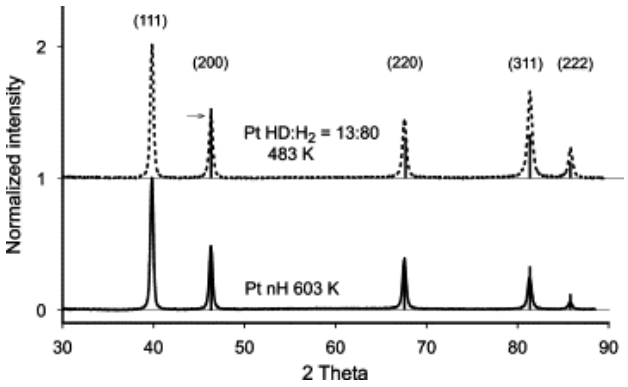

Fig. 3. X-ray diffraction pattern of PtN after two different treatments. The relative intensities for a bulk Pt (JPCDS file 04-0802) are shown with vertical lines below each peak. The arrow points to the maximum intensity of the (2 0 0) peak on the upper curve. The anisotropic rearrangement after the treatment with 2,4HD═/H_2 at 483 K is clearly seen.

3.2. Transformations of the deactivating hydrocarbons

Table 2 shows the transformation of the hydrocarbon applied during deactivation runs, expressed as turnover frequencies (TOF, h^{-1}). Relatively low (almost temperature-independent) values were observed after *n*H treatments of PtN while the reaction of hexadiene was much more rapid. Fig. 4 shows the corresponding product selectivities with *n*H and 2,4HD═ for PtN. The products of all "skeletal" reactions [13] and [14] (isomerization/C_5-cyclization, aromatization, and hydrogenolysis) appeared from hexane at each temperature. The amount of isomers decreased rapidly, methylcyclopentane (MCP) increased from 483 to 543 K. Both dropped almost to zero at 663 K. The selectivity towards benzene formation as well as towards hexenes increased, at the same time, the selectivity of fragments was almost unchanged. Hexadiene was hydrogenated with nearly 100% selectivities to hexane at 483 and 543 K. The main products were hexenes and double-bond hexadiene isomers at 603 and 663 K. The benzene selectivity was smaller but, due to the higher TOF, its yield was much more than from hexane.

Table 2: Turnover frequencies (TOF, h^{-1}) in pretreating exposures of different catalysts (t = 20 min)

Temperature (K)	PtN	EPT	Pt/GNF-H	Pt/CeO_2
Treatment: hexane				
483	0.7	2	1.8	0.63
543	3.6	4.8	11	–
603	3.9	7.5	13	4.2
663	3.4	11.2	14	–
603, no H_2	1.0	2.3	8.5	–
Treatment: hexadiene				
483	50	55	112	74
543	49	54	112	–
603	44	53	111	27
663	20	50	101	12

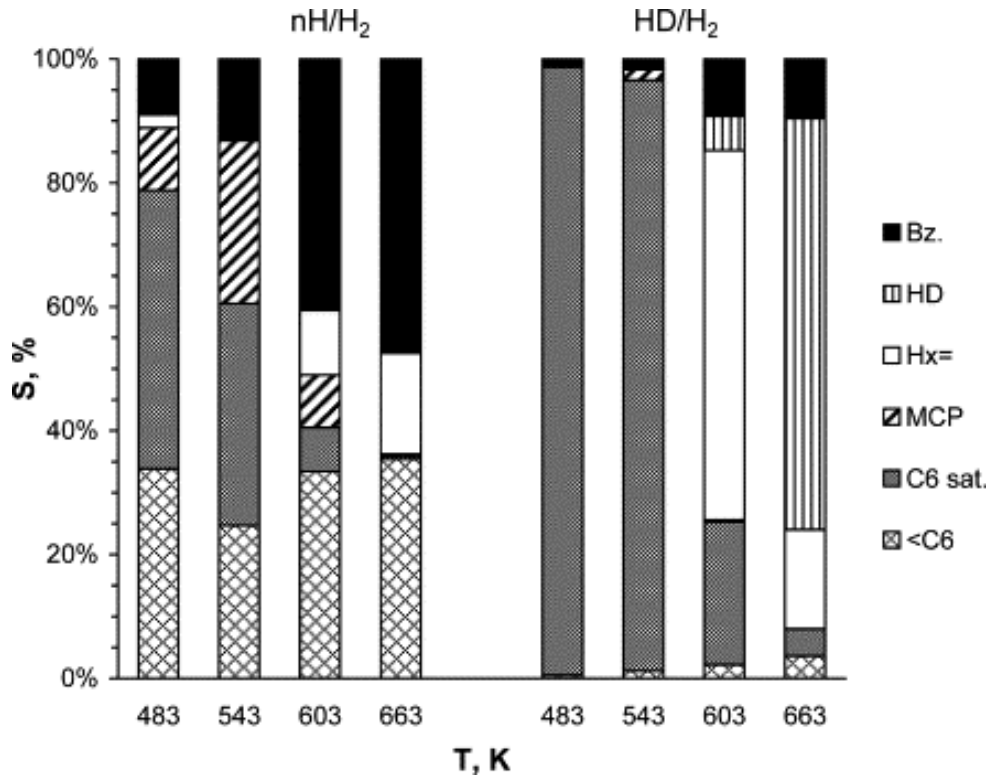

Fig. 4. Selectivities observed in the reaction of the deactivating hydrocarbon (13 mbar *n*H or 2,4HD⩵, 80 mbar H_2) during its contact of 20 min with the PtN catalyst at four temperatures. (<C_6: fragments: C_6 sat.: isohexanes from *n*H; *n*-hexane plus isohexanes from 2,4HD⩵).

Table 3: Selectivities observed in the reaction of the deactivating hydrocarbon (13 mbar *n*H or 2,4HD⩵, 80 mbar H_2) during its contact of 20 min with the three supported Pt catalysts at selected temperatures. C_6 saturated products represents hexane isomers in the case of hexane transformation and mainly hexane in the case of hexadiene transformation

Hydrocarbon	EUROPT-1			Pt/GNF			Pt/CeO_2		
	T = 483 K	*T* = 603 K		*T* = 483 K	*T* = 603 K		*T* = 483 K	*T* = 603 K	
	*n*H	*n*H	2,4HD=	*n*H	*n*H	2,4HD=	*n*H	*n*H	2,4HD=
<C6	3.6	12	1.2	17.6	11.7	2.0	40.7	43.4	15.9
C_6 saturated	47.4	15.6	90.3	39.5	18.1	82.3	24.7	13.9	65.5
MCP	45.3	36.9	4.8	40.6	51.7	5.4	32.7	14.2	7.8
Hexenes	0	8.8	0.4	0	1.3	6.5	0	0.0	1.9
Benzene	3.7	26.7	3.3	2.3	17.2	3.8	1.9	28.5	9

The TOF values for EUROPT-1 and Pt/GNF-H in hexane reactions were larger than that for PtN (Table 2), while those for Pt/CeO_2 were to almost identical to those measured for unsupported Pt. With hexadiene feed, in turn, PtN and EUROPT-1 resulted in similar transformation rates and the values for Pt/GNF-H were about twice as high.

Selectivity values for supported Pt catalysts at selected temperatures are shown in Table 3. The qualitative changes of the selectivities of *n*H reactions is similar to that shown in Fig. 4 for PtN. The quantitative values are, however, different. Much more saturated C_6 hydrocarbons were formed from *n*H over both EUROPT-1 and Pt/GNF-H, even at 603 K where their amount showed an abrupt drop on PtN. Similarly, the predominance of hexane formation from 2,4HD⩵ still appeared at 603 K. The selectivity patterns at 663 K (not shown) were very close, however, to those observed on PtN, except that less benzene and more hexene were found on the supported catalysts. Pt/CeO_2 produced more fragments than any other sample, but no hexenes were formed at all from *n*H. This catalyst could, however, hydrogenate 2,4HD⩵ to hexenes. More methylcyclopentane was observed on this catalyst than on Pt/N.

3.3. Activities and selectivities in standard test runs

The activities (expressed as TOF, h^{-1}) in standard test runs for the four regenerated catalysts are shown in Table 4. Pt/GNF-H proved to be the most active catalyst, exceeding the performance of EUROPT-1 [39]. Longer reaction times led to decrease of TOF values in the test runs, so-called "self-deactivation". Most catalysts lost about one half of their initial activity after 20 min

Table 4: Comparison of different catalysts in standard test runs over regenerated catalysts[a]

Catalyst:	Activity (TOF_0, h^{-1})			
	5 min	20 min	35 min	50 min
PtN	20 ± 0.8[b]	9.5	6.8	5.5
Pt–HCHO	18	8	6	4.8
EUROPT-1	30	17	12	9.5
Pt/GNF-H	52	24	17	13
Pt/CeO_2	6.5	23	16	13

[a] Test run: $p(n\text{H}):p(\text{H}_2)$ = 13:160 mbar; T = 603 K, 50 min.
[b] Average of 21 runs, Ref. [7].

(Table 4). The TOF values averaged over 50 min were around 1/3–1/4 of the initial ones. Pt/CeO_2 was a conspicuous exception: here the TOF belonging to 20 min increased considerably compared to the initial value. A great fraction of hydrogen is used up probably in a spillover process which can be irreversible here [40], since hydrogen is utilized for reduction of the ceria support in the vicinity of Pt particles. Thus, fewer active sites are available for reaction on the hydrogen-lean Pt surface. Having completed this reduction, hydrogen will be used for maintaining the active state of Pt. The intermediate TOF values measured after 20 and 35 min showed, therefore, a deactivation somewhat smaller than in other cases.

The residual activity (TOF/TOF_0) after different carbonizing pretreatments is shown in Table 5 for all catalysts. Corresponding selectivity values at t = 5 min are presented in Fig. 5a for unsupported PtN. Many fragments (≃40%) were formed on PtN, with almost uniform selectivities towards isomers, MCP and benzene. The selectivities over samples pretreated with $n\text{H}/\text{H}_2$ were close to the values found on regenerated Pt up to 603 K pretreatment temperature. The hexene selectivity increased sharply after the pretreatment at 663 K. This was still more marked after deactivation with nH alone at 603 K. The abrupt shift of the selectivity pattern (the drop of "hydrogenative" reactions) started at much lower temperature (≃543 K) after $2,4\text{HD}{=\!=}/\text{H}_2$. Note that benzene selectivity was almost constant, except for the high value after $2,4\text{HD}{=\!=}/\text{H}_2$ at 663 K. This latter treatment suppressed every reaction except for dehydrogenative processes. The pronounced change of the selectivity pattern (between 603 and 663 K) was parallel to the spectacular drop of the total activity (Table 5) after deactivation with nH. A similar abrupt activity drop took place between 483 and 543 K after $2,4\text{HD}{=\!=}$ pretreatment (Table 5) but the selectivity changes were more gradual in this temperature range.

The activity decrease at increasing temperature was less dramatic on supported Pt catalysts (Table 5). Fig. 5b shows an analogous compilation for EUROPT-1. The differences are conspicuous. The main products were MCP and isomers with much less fragments [20] and [23]. Deactivation slightly increased the MCP selectivity at the expense of isomerization. Almost equal selectivity patterns were

Table 5: Residual activity (TOF/TOF_0) of various catalysts in hexane test reaction after different pretreatments[a]

T (pretr.)	PtN	EPT		PtGNF-H		Pt/CeO_2
Sampling time	5 min	5 min	50 min	5 min	50 min	5 min
Pretreatment: hexane						
483	0.75	0.70	0.76	0.81	0.89	0.94
543	0.80	0.70	0.72	0.69	0.82	–
603	0.59	0.73	0.74	0.51	0.54	0.74
663	0.18	0.58	0.63	0.31	0.39	0.53
603 (no H_2)[b]	0.10	0.39	0.50	0.17	0.31	–
Pretreatment: *trans-trans*-hexa-2,4-diene						
483	0.63	0.75	0.77	0.76	0.79	1.05
543	0.18	0.68	0.69	0.46	0.63	–
603	0.16	0.70	0.71	0.32	0.52	0.69
663	0.15	0.47	0.52	0.17	0.22	0.39

[a] Pretreatment: $p(n\text{H}):p(\text{H}_2)$ = 13:80 mbar and $p(24\text{HD}{=\!=}):p(\text{H}_2)$ = 13:80 mbar; t = 20 min; TOF/TOF_0 values are shown, measured in test runs [$p(n\text{H}):p(\text{H}_2)$ = 13:160 mbar; T = 603 K] on regenerated catalyst (TOF_0) and after deactivating pretreatment (TOF).
[b] Pretreatment: $p(n\text{H})$ = 53 mbar.

observed after deactivations with nH and $2,4\text{HD}{=\!=}$. A stronger change occurred – after deactivation with both hydrocarbons – at 663 K only, but it was less spectacular than the effect observed on PtN (cf. Fig. 6a and b).

Table 6 summarizes selected results for other supported samples: Pt/GNF-H and Pt/CeO_2. MCP was the main product on the graphite nanofiber supported platinum. Its pronounced isomerization activity manifested itself at lower temperatures and higher hydrogen pressures [32] and [39], but the low aromatization selectivity still persevered. In spite of the significant loss of activity (Table 5), the selectivity pattern after deactivating runs changed very little: MCP increased at the expense of isomers and very small amounts of hexenes appeared after severe pretreatments. The behavior of Pt/CeO_2 is exceptional. The activity did not drop so spectacularly after pretreatments (Table 5). Deactivation suppressed the very high fragmentation selectivity with a simultaneous increase of some of the non-degradative products: MCP and isomers. No hexenes were produced, except for traces in one case.

The TOF values decreased as a function of time over the carbonized samples, similar to that observed after regeneration (Table 4). This change, however, was less pronounced on the deactivated samples and thus the residual activity (expressed in (TOF/TOF_0) × 100) increased (Table 5). We called this process "self re-activation" [6] and [7] caused most probably by the higher hydrogen content in the standard test run than in the deactivating pretreatments. Fig. 6 depicts results from one selected example: PtN deactivated at 603 K: the residual activity (TOF/TOF_0) was ≃60% after pretreatment with $n\text{H}/\text{H}_2$ and remained so after 50 min. The TOF/TOF_0 value of 0.16 after 5 min of the test run following $2,4\text{HD}{=\!=}$ treatment at 603 K increased to 0.23 after 50 min. Hardly any selectivity changes were observed after contact with $n\text{H}/\text{H}_2$, MCP somewhat increasing, fragmentation and isomerization decreasing. The same was seen on a bigger scale after $2,4\text{HD}{=\!=}/\text{H}_2$

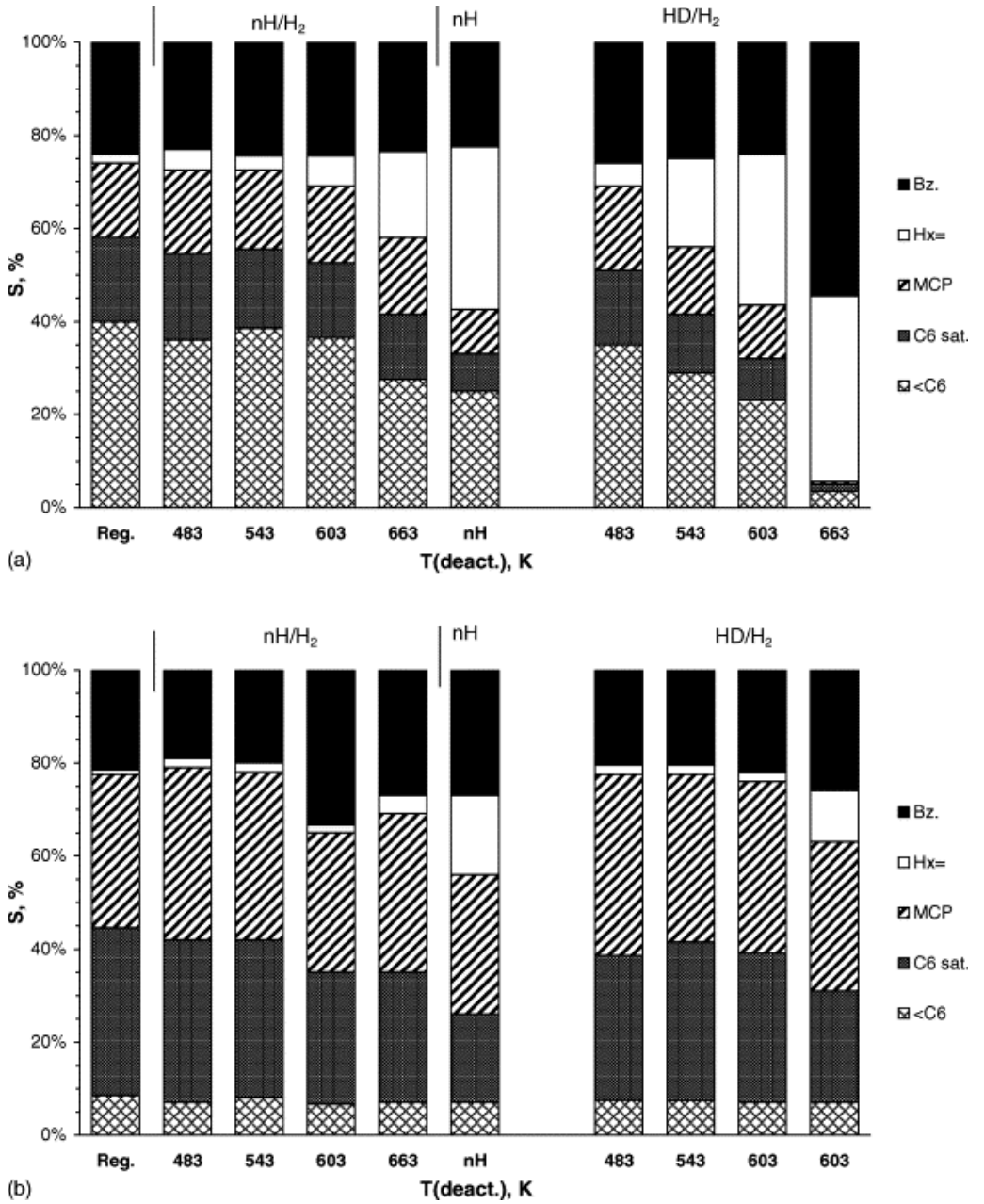

Fig. 5. Selectivities observed in standard test runs (p(*n*H):p(H_2) = 13:160 mbar; T = 603 K, t = 5 min) on regenerated Pt as well as after deactivation with *n*H alone (603 K), with *n*H/H_2 and 2,4HD═/H_2 mixtures at different temperatures, p(*n*H or 2,4HD═):p(H_2) = 13:80 mbar. The temperatures of pretreatments are given on the abscissa; "Reg." means regenerated catalyst, "*n*H": pretreatment with *n*H alone, T = 603 K. (a) Pt black (PtN); (b) EUROPT-1.

Table 6: Selectivities observed in test runs – p(*n*H):p(H_2) = 13:160 mbar; T = 603 K, t = 5 min – on regenerated (reg.) Pt/GNF and Pt/CeO_2 catalysts as well as after deactivation with *n*H alone, with *n*H/H_2 and 2,4HD═/H_2 mixtures at different temperatures. p(*n*H or 2,4HD═):p(H_2) = 13:80 mbar was applied during deactivation

Treatment	Pt/GNF						Pt/CeO_2					
	Reg.	*n*H/H_2		*n*H	2,4HD=/H_2		Reg.	*n*H/H_2		2,4HD=/H_2		
	T = 603 K	T = 483 K	T = 603 K	T = 603 K	T = 483 K	T = 603 K	T = 603 K	T = 483 K	T = 603 K	T = 483 K	T = 603 K	T = 663 K
<C6	12.5	12.5	12	15	12.5	13	64	55	43.5	43	34	29
C_6 saturated	30.5	25	21.5	16	25.5	18.5	8.5	15	15.5	19.5	18	13
MCP	44	49	54	55	48.5	55	5	6.5	27	13	31	33
Hexenes	0	0.5	0.5	2	0.5	0.5	0	0.5	0	0.5	0	0
Benzene	13	13	12	12	13	13	22.5	19	14	24	17	25

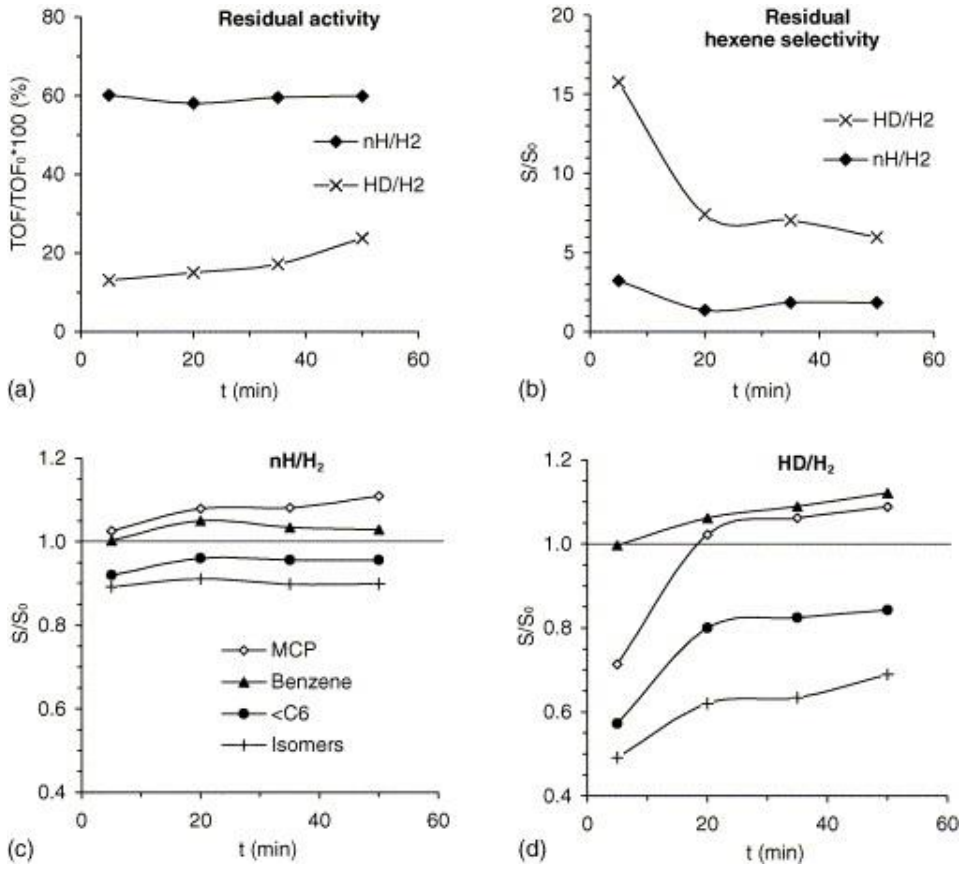

Fig. 6. Activity and selectivity changes during the standard test runs of 50 min on PtN catalyst after treatments by hexane–hydrogen (nH/H_2) or by hexadiene–hydrogen (2,4HD═/H_2) respectively, at T = 603 K, p(nH or 2,4HD═):p(H_2) = 13:80 mbar. (a) Residual activity; (b) residual selectivity of hexene formation (S/S_0); (c) other S/S_0 values after hexane–hydrogen (nH/H_2) treatment; (d) other S/S_0 values after hexadiene–hydrogen (2,4HD═/H_2) treatment. The same signs are used in c and d.

pretreatment, the S/S_0 values of benzene and MCP exceeding even unity. The hexene selectivity increased up to two times after nH/H_2, as opposed to the increase of up to 15 times caused by 2,4HD═/H_2. The drop of S/S_0 for hexenes to values of 6–7 after 20 min of the test run permitted some other selectivities to increase (Fig. 6b and d).

4. Discussion

4.1. Pt black: correlation between catalytic pattern and surface state

The most complete picture was obtained with platinum black. This "classical" catalyst [6], [7] and [41] has at present little practical importance, but it permitted us to compare activity changes with studies by electron spectroscopy as well as by X-ray diffraction [7].

Carbon on the regenerated (active) catalysts (minimum ∼10%, Table 1) may correspond to the "invisible" or "harmless" carbon postulated by Menon [42]. The reappearance of surface C upon hydrogen treatment was reported earlier [7]. The amount of carbon was more at higher temperature and with 2,4HD═ as deactivating agent and increased up to 40–45%. There was no straight correlation between the larger carbon percentage and deactivation. The plot of the activity loss as a function of the actual carbon percentage (Fig. 7) shows two groups of points with rather wide scatter. The data corresponding to nH/H_2 treatments at 483, 543 and 603 K, as well as to 2,4HD═/H_2 at 483 K indicate minor deactivation with gradual increase of the C content from 12 to 15% up to ∼30%. The pretreatment at 663 K with nH/H_2 did not involve any further increase of the C % nevertheless, more than 75% of the initial activity was lost. Other treatments with 2,4HD═/H_2 and those in the absence of H_2 increased the C% above 50% with a slow further activity loss reaching ∼8% residual activity. Data points taken from an earlier study with Pt–HCHO [6] (e. g. that showing 53% C) harmonize well with results of PtN.

Not only the amount of carbon but also its chemical state is important for deactivation [6]. Fig. 7 shows an abrupt change in the residual activities above 603 K with nH/H_2 and already at 543 K with 2,4HD═/H_2 (Table 5). This is the range, where the activity loss became almost independent of the C%. The XPS difference curves show the appearance of a C 1s component at 284.1 eV from 2,4HD═ in this range, confirmed also by the UPS results

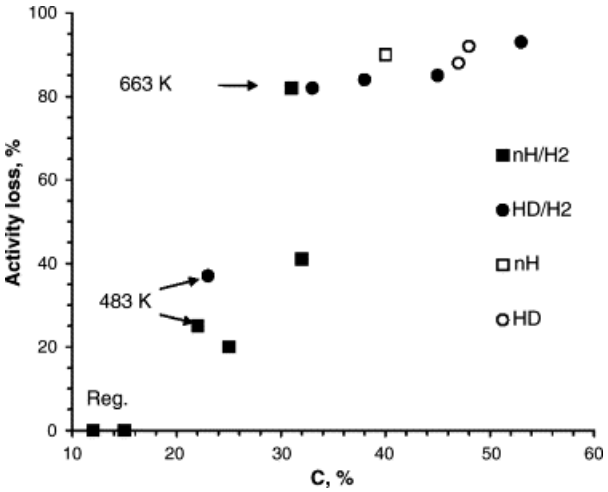

Fig. 7. Activity loss in test runs as a function of the C%, measured by XPS on PtN (Table 1). The three points on the far right, one concerning 2,4HD═/H_2, two 2,4HD═ treatment have been measured with Pt–HCHO [6].

(Fig. 1 and Fig. 2). This component was identified as a "disordered" carbonaceous deposit [1], representing, very likely, a branched, non-graphitic surface polymer with several Pt—C bonds and was regarded as responsible for major deactivation [6]. Its excess, however small, after 2,4HD═ treatments at 603 K caused a pronounced selectivity change (Fig. 5a), poisoning first of all hydrogenative reactions. At 663 K, the massive graphitization deactivated Pt to similar extent after both treatments but the additional carbon (including graphite) after 2,4HD═/H_2 killed almost totally every selectivity except that of dehydrogenation. Pt black after deactivation with *n*H/H_2 at 663 K showed a selectivity pattern similar to that found after 2,4HD═/H_2 at 543 K (Fig. 5a). Identical selectivity patterns appeared after deactivation at 603 K, both with *n*H alone and 2,4HD═/H_2 (Fig. 5a), although the *activity loss* was stronger with *n*H alone (Table 5). The UP spectra showed a marked Fermi-edge even after the most severe pretreatment. The metallic Pt sites still available may have included a few three-atom Pt ensembles necessary to form benzene [43], even when ~90% of the activity was lost.

The analysis after the deactivating runs (Table 4, Fig. 5) is rather informative. Much isomers and MCP were formed at 483 and 543 K on hydrogen-rich Pt sites [13], [14] and [44] with the loss of at least one H-atom, forming a Pt—C bond. The gradual disappearance of these products at higher temperatures indicates that further, multiple dissociation occurred, preceding carbon formation by polymerization of unsaturated intermediates with *trans*-structure [45]. Hexadiene, in turn, was hydrogenated almost completely to hexane at 483 and 543 K. This reaction did *not* require the formation of C—Pt bonds, considering that π-bonded intermediates [46] and, at least partly, subsurface hydrogen [47] participated in double-bond hydrogenation. This reaction took place parallel to the polymerization of *trans*-hexadienes to "coke precursors" [13] at 543 K (cf. Fig. 4 and Fig. 5a). Most reactions to saturated products stopped at higher temperatures.

A close correlation was reported between the carbon and hydrogen coverage of Pt catalysts during hydrocarbon reaction [16]. This is a mutual interrelationship: much hydrogen can prevent deactivation, much carbon displaces surface hydrogen and contributes also to catalyst restructuring (Fig. 3). Considering that hydrogen-rich conditions [13] – and rough surfaces favored by much hydrogen [16] – are needed for the C_5-cyclic route of saturated product formation, it explains why carbonization hampered first of all isomerization and C_5-cyclization.

4.2. Supported Pt catalysts: a generalized model

The above principles can explain *mutatis mutandis* the behavior of supported Pt catalysts. Two factors can cause differences: (1) the smaller metal particles of the supported catalysts and (2) the possibility of hydrogen spillover to the support and back-spillover to Pt.

(1) Small Pt particles do not favor polymerization of dehydrogenated "coke precursors" [18]. This can be the reason why the activity loss was much milder on all supported Pt than on Pt black (Table 5). In fact, two different coke formation routes were described [48]: on supported catalysts, with high dispersion, carbonaceous deposits could be formed through C_1 intermediates ("C_1-route"), while on Pt black samples the "polyene-route", i.e. polymerization of unsaturated precursors can prevail. EUROPT-1 retained as little as 0.3–0.5 C/Pt_s between 453 and 593 K, as opposed to the higher values with Pt black [49]. Furthermore, the carbonaceous deposits contained more H on EUROPT-1 (H/C = 1.0–1.6), than on Pt black (H/C = 0.4–1) [18]. Considering the cubooctahedron model of Pt on EUROPT-1 [23] and [50], its small (1 1 1) facets are suitable for benzene formation while two-atom ensembles for C_5-cyclic reactions are present on both (1 1 1) and (1 0 0) facets [23] as well as on stepped sites [11] and [12]. These sites seemed to deactivate almost uniformly, as seen from the minor changes in selectivity (Fig. 5b). The same can be stated for Pt/GNF-H (Table 6).

(2) Hydrogen spillover in both directions contributes considerably to the catalytic propensities. Back-spillover increasing the "virtual hydrogen pressure" on the Pt sites [20] and [22] contributes to lower deactivation (hydrogenation rather than polymerization of poly-unsaturated "coke precursors"). This favors the formation of isomers and MCP from hexane [20] and saturated products from hexadiene (Table 3). Due to the hydrogen storage capacity of the graphite nanofiber support [51], their amount was highest over Pt/GNF-H. Commencing deactivation of these supported Pt samples did not poison C_5-cyclic reactions but their common surface product [14] desorbed preferentially as MCP at the expense of skeletal isomers.

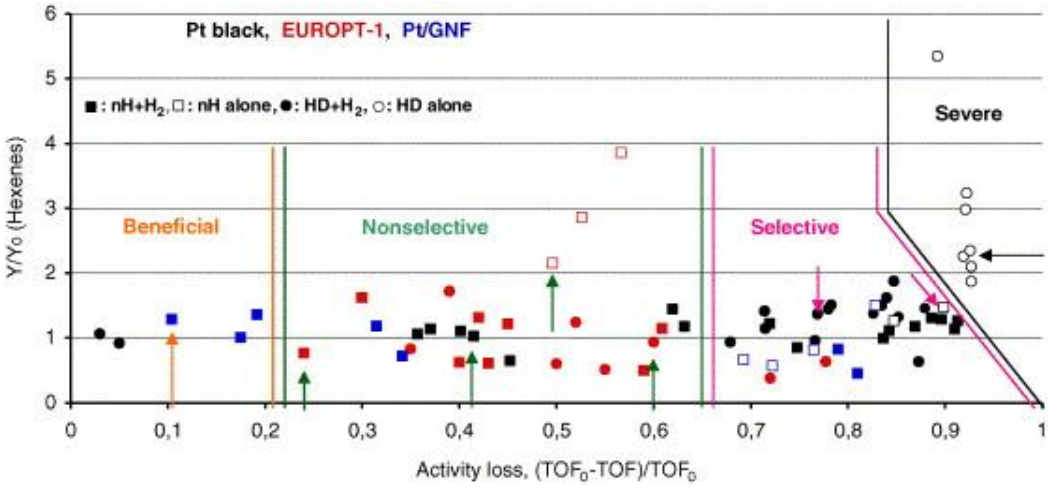

Fig. 8. Correlation between the yield of hexenes and the activity loss in test runs after different pretreatments of Pt black, EUROPT-1 and Pt/GNF-H. Selectivities belonging to selected points (arrows) are shown inTable 7.

Table 7: Activity loss ($TOF_0 - TOF)/TOF_0$ and selectivity change (S/S_0) values for different catalysts in test run ($p(n\text{H}):p(\text{H}_2)$ = 13:80 mbar, T = 603 K) after deactivation treatments corresponding to selected points in Fig. 8

Region	Beneficial	Non-selective				Selective		Severe
Catalyst (treatment)	Pt/GNF-H (nH–H_2, 483 K)	EUROPT-1 (nH–H_2, 483 K)	PtN (HD–H_2, 603 K)	EUROPT-1 (nH, 603 K)	EUROPT-1 (HD–H_2, 603 K)	Pt-HCHO (HD–H_2, 663 K)	PtN (nH, 603 K)	Pt-HCHO (HD–H_2, 693 K)
$(TOF_0 - TOF)/TOF_0$	0.1	0.24	0.42	0.49	0.60	0.76	0.90	0.93
S/S_0								
Fragments	1.01	0.96	0.96	0.78	0.84	0.76	0.63	0.51
Isomers	0.87	1.05	0.90	0.71	0.88	0.70	0.46	0.32
Hexenes	1.43	1.01	1.84	4.28	2.34	5.92	16.84	31.72
MCP	1.09	1.00	1.11	1.10	1.12	0.98	0.59	0.60
Benzene	1.12	0.95	1.03	1.23	1.02	1.02	0.92	1.01

Hexenes represent the only product class, the selectivity of which always increased on deactivated catalysts [6] and [23]. Considering also the overall activity loss, the hexene *yields* ($Y = S \times X$) remained considerably stable on partly deactivated catalysts. Four regions of deactivation can be distinguished: I, beneficial; II, non-selective; III, selective; IV, severe deactivation. These regions are depicted in Fig. 8, using the same symbols for Pt blacks as in Fig. 7. Selectivity changes corresponding to selected points are shown in Table 7. Supported Pt catalysts and Pt black showed similar selectivity values at analogous activity loss. "Beneficial" deactivation can mean the formation of "Pt–C–H" system favoring the formation of saturated C_6 products at the expense of fragmentation [2]. Treatments with 2,4HD=/H_2 at 483 K belong to this class (Table 7), where XPS (Fig. 1) showed different types of surface carbon. The increased amount of high Miller-index sites observed by XRD (Fig. 3) indicates that this catalyst represented a "hydrogen-rich" system (7, 10). The majority of points in the "non-selective" region belong to measurements on supported Pt catalysts where deactivation was not too strong and the selectivity pattern did not change dramatically, either (Table 7). The treatments of Pt black at higher temperatures, causing a stronger activity loss (cf. Table 6), belong to the region of "selective" deactivation (poisoning mainly isomerization), with still similar hexene yields, although the scattering is much larger here. The accumulation of the "disordered" carbon (C 1s BE ~284.1 eV) starts in this region and becomes preponderant in the region of "severe" deactivation (Fig. 1). Only Pt black reached this state [6]; with carbon percentages as high as 45–50% (Fig. 7). This sample must have transformed into the deactivated "Pt–C" state [2] and [49]. Dehydrogenation may have been catalyzed by PtC ensembles and/or by single Pt atoms [23] and [52].

The hexene yield on EUROPT-1 after pretreatments with nH alone increased well above unity after the loss of about half of the original activity (Fig. 8). These points also belonged to the "non-selective" region according to the selectivity changes (Table 7). The larger grains of Pt/GNF-H were similar to Pt black but hydrogen back-spillover must have prevented extensive carbonization. Pt/CeO_2 represented a class of its own, since it produced no hexenes. The explanation lies, likely in the spillover process. Most of the hydrogen migrating to the ceria support [40] is used up for reduction of Ce^{IV} to Ce^{III} rendering back-spillover impossible. Insufficient H on Pt sites causes a low initial activity (Table 4). It increased after reducing ceria

sites surrounding the Pt particles. At the same time spillover and back-spillover of oxygen can also take place [53], and this oxygen reportedly contributes to CO oxidation on Pt sites [54] and [55]. It is logical to assume that the lack of hexenes is due to oxidation of their chemisorbed precursors. This supposition needs further confirmation. Removal of unsaturated surface entities means slower accumulation of the "useful" carbon necessary for non-degradative reactions as opposed to hydrogenolysis [2], leading to *increased* selectivities of isomerization–C_5-cyclization (Table 3) after pretreatments causing their decrease in other cases (Fig. 5, Table 6). At the same time, these treatments caused the decrease of the overall activity of Pt/CeO_2, too.

5. Conclusion

Monofunctional catalysts were intentionally deactivated with two hydrocarbons: hexane (*n*H) and 2,4-hexadiene (24HD$=\!=$). The catalysts included (1) Pt black with larger particles but permitting electron spectroscopy of "fresh" and "deactivated" samples [7] and [34]; (2) EUROPT-1 (6% Pt/SiO_2) with small cubooctahedral crystallites [24]; (3) Pt–graphite nanofiber (Pt/GNF-H) where the support had a hydrogen storage ability [32]; (4) Pt/CeO_2 where the reduction ($Ce^{IV} \rightarrow Ce^{III}$) consumed spilt over hydrogen [26]. The deactivating exposures were carried out between 483 and 663 K without H_2 or in six-fold H_2 excess. The transformation of the hydrocarbon during deactivating run was monitored and the residual activity was checked in "standard test runs" (603 K, *n*H:H_2 = 13:160 mbar).

The activity loss was parallel but not strictly proportional to the C% shown by XPS (22–45% as opposed to ca. 10% on regenerated Pt black). The chemical state of the deposited carbon may have been the main factor determining deactivation: "disordered carbon" (BE ≃284.1 eV) and, to a lesser extent, graphitic (BE ≃284.6 eV) and C_xH_y polymers (BE ≃285.6 eV) being its primary cause. XPS difference spectra show that at $T \geq 603$ K more of these species accumulated, particularly from 24HD$=\!=$. Accordingly, deactivation was rather small after low-temperature treatments and increased abruptly at $T \geq 603$ K. This was concomitant with spectacular selectivity changes in deactivating runs: isomerization of *n*H dropped markedly and dehydrogenation increased. 24HD$=\!=$ was hydrogenated to hexane at low temperature but gave mostly hexenes and hexadiene isomers at $T \geq 603$ K. Much less of the "massive" carbon species was formed after treatment with 24HD$=\!=$ at 473 K in excess H_2, where its p-bonded chemisorption prevailed.

No high-molecular contiguous carbon deposits could be formed on the smaller Pt particles of supported catalysts, thus the activity and selectivity changes were less pronounced, especially at higher temperatures. Hydrogen spillover could also be important factor determining the less significant deactivation of supported Pt. Accordingly, Pt/GNF showed lower deactivation than EUROPT-1. The hexene yields on these catalysts provided a general factor for characterizing the state of the deactivation. Pt/CeO_2 was an exception, producing no hexenes but more fragments in the standard test and could regain some activity in longer runs.

Acknowledgement

The work has been supported partly by the Hungarian National Science Foundation, Grant OTKA T37241. Z.P. thanks the Max-Planck-Gesellschaft, A.W. the Bolyai Grant of the Hungarian Academy of Sciences for additional financial support. The authors are grateful to Dr. R. T. K. Baker and Dr. N. M. Rodriguez for supplying the graphite nanofiber support, to Dr. Ágnes Mastalir (University of Szeged) for the synthesis of the Pt/GNF-H catalyst, as well as to Dr. Josef Find for the X-ray diffraction measurement.

References

[1] G.A. Somorjai and F. Zaera, *J. Phys. Chem.* **86** (1982), p. 3070.
[2] A. Sárkány, *J. Chem. Soc., Faraday Trans. 1* **84** (1988), p. 2267.
[3] F. Garin, G. Maire, S. Zyade, M. Zauwen, A. Frennet and P. Zielinski, *J. Mol. Catal.* **58** (1990), p. 185.
[4] G. Webb, *Catal. Today* **7** (1990), p. 139.
[5] Z. Paál and Z. Zhan, *Langmuir* **13** (1997), p. 3752.
[6] N.M. Rodriguez, P.E. Anderson, A. Wootsch, U. Wild, R. Schlögl and Z. Paál, *J. Catal.* **197** (2001), p. 365.
[7] Z. Paál, U. Wild, A. Wootsch, J. Find and R. Schlögl, *Phys. Chem. Chem. Phys.* **3** (2001), p. 2148.
[8] G.A. Somorjai, *Catal. Lett.* **12** (1992), p. 17
[9] G.A. Somorjai, *J. Mol. Catal. A: Chem.* **107** (1996), p. 39.
[10] J. Find, Z. Paál, R. Schlögl and U. Wild, *Catal. Lett.* **65** (2000), p. 19.
[11] F. Garin, S. Aeiyach, P. Légaré and G. Maire, *J. Catal.* **77** (1982), p. 323
[12] A. Dauscher, F. Garin and G. Maire, *J. Catal.* **105** (1987), p. 233.
[13] Z. Paál, *Adv. Catal.* **29** (1980), p. 273.
[14] F.G. Gault, *Adv. Catal.* **30** (1981), p. 1.
[15] G. Maire, F. Bernhardt, P. Légaré and G. Lindauer, *Proceedings of the Seventh International Vacuum Congress and Third International Conference on Solid Surfaces* Vienna (1977), p. 861.
[16] P. Légaré and F. Garin, *J. Catal.* **214** (2003), p. 336.
[17] G.C. Bond, *Appl. Catal. A: Gen.* **191** (2000), p. 23.
[18] A. Wootsch, C. Descorme, Z. Paál and D. Duprez, *J. Catal.* **208** (2002), p. 273.
[19] Z. Paál In: Z. Paál and P.G. Menon, Editors, *Hydrogen Effects in Catalysis*, Dekker, New York (1988), p. 449.

[20] (a) A. Wootsch and Z. Paál, *J. Catal.* **185** (1999), p. 192. (b) A. Wootsch and Z. Paál, *J. Catal.* **205** (2002), p. 86.
[21] Z. Paál, G. Székely and P. Tétényi, *J. Catal.* **58** (1979), p. 108.
[22] J.A. Biscardi and E. Iglesia, *J. Catal.* **182** (1999), p. 117.
[23] Z. Paál, H. Groeneweg and J. Paál-Lukács, *J. Chem Soc., Faraday Trans.* **86** (1990), p. 3159.
[24] G.C. Bond and Z. Paál, *Appl. Catal. A: Gen.* **86** (1992), p. 1.
[25] N.M. Rodriguez, A. Chambers and R.T.K. Baker, *Langmuir* **11** (1995), p. 3862.
[26] D. Teschner, A. Wootsch, T. Röder, K. Matusek and Z. Paál, *Solid State Ionics* **141–142** (2001), p. 709.
[27] Z. Paál, A. Wootsch, K. Matusek, U. Wild and R. Schlögl, *Catal. Today* **65** (2001), p. 13.
[28] Z. Paál and A. Wootsch In: S.D. Jackson, J.S.J. Hargreaves and D. Lennon, Editors, *Catalysis in Application*, The Royal Society Chemistry, Cambridge (2003), p. 8.
[29] J. Find, Z. Paál, H. Sauer, R. Schlögl, U. Wild and A. Wootsch In: A. Corma *et al.*, Editors, *Stud. Surf. Sci. Catal.* **130**, Elsevier, Amsterdam (2000), p. 2291.
[30] C. Paal, *Berichte* **49** (1916), p. 548.
[31] N.M. Rodriguez, A. Chambers and R.T.K. Baker, *Langmuir* **11** (1995), p. 3862.
[32] R.T.K. Baker, N.M. Rodriguez, Á. Mastalir, U. Wild, R. Schlögl, A. Wootsch and Z. Paál, *J. Phys. Chem. B* **108** (2004), p. 14348.
[33] In: D. Briggs and M.P. Seah, Editors, *Practical Surface Analysis* **vol. 1**, Wiley, Chichester (1990), p. 635 Appendix 6.
[34] Z. Paál, R. Schlögl and G. Ertl, *J. Chem. Soc., Faraday Trans.* **88** (1992), p. 1179.
[35] Z. Paál, R. Schlögl and G. Ertl, *Catal. Lett.* **12** (1992), p. 297.
[36] J.R. Behm, Ph.D. Thesis, University of München, 1983.
[37] Sh.K. Shaikhutdinov, M. Frank, M. Bäumer, S.D. Jackson, R.J. Oldman, J.C. Hemminger and H.-J. Freund, *Catal. Lett.* **80** (2002), p. 115.
[38] Z. Paál, K. Matusek and M. Muhler, *Appl. Catal. A: Gen.* **149** (1997), p. 113.
[39] R.T.K. Baker, K. Laubernds, A. Wootsch and Z. Paál, *J. Catal.* **193** (2000), p. 165.
[40] S. Bernal, J.J. Calvino, G.A. Cifredo, J.M. Gatica, J.A.P. Omil and J.M. Pintado, *J. Chem. Soc., Faraday Trans.* **89** (1993), p. 3499.
[41] D.J. O'Rear, D.G. Löffler and M. Boudart, *J. Catal.* **94** (1985), p. 225.
[42] P.G. Menon, *J. Mol. Catal.* **59** (1990), p. 207.
[43] P. Biloen, J.N. Helle, H. Verbeek, F.M. Dautzenberg and W.M.H. Sachtler, *J. Catal.* **63** (1980), p. 112.
[44] Z. Paál In: G.J. Antos and A.M. Aitani, Editors, *Catalytic Naphtha Reforming* (2nd ed. (revised and expanded)), Marcel Dekker, New York (2004), p. 35.
[45] Z. Paál and P. Tétényi, *J. Catal.* **30** (1973), p. 350.
[46] G. Rupprechter and G.A. Somorjai, *J. Phys. Chem. B* **103** (1999), p. 1623.
[47] Sh. Shaikhutdinov, M. Heemeier, M. Bäumer, T. Lear, D. Lennon, R.J. Oldman, S.D. Jackson and H.-J. Freund, *J. Catal.* **200** (2001), p. 330.
[48] A. Sárkány, H. Lieske, T. Szilágyi and L. Tóth, *Proceedings of the Eighth International Congress on Catalysis, vol.2* Berlin (1984), p. 613.
[49] A. Sárkány, *Catal. Today* **5** (1989), p. 173.
[50] V. Gnutzmann and W. Vogel, *J. Phys. Chem.* **94** (1990), p. 4991.
[51] C. Park, P.E. Anderson, A. Chambers, C.T. Tan, R. Hidalgo and N.M. Rodriguez, *J. Phys. Chem. B* **103** (1999), p. 10572.
[52] V. Ponec, *Adv. Catal.* **32** (1983), p. 149.
[53] S. Salasc, V. Perrichon, M. Primet, M. Chevrier and N. Mouad-dib-Moral, *J. Catal.* **189** (2000), p. 401
[54] T. Bunluesin, R.J. Gorte and G.W. Graham, *Appl. Catal. B: Environ.* **15** (1998), p. 107.
[55] S. Bedrane, C. Descorme and D. Duprez, *Catal. Today* **73** (2002), p. 233.